# Effect of Plasticizer on the Electrical, Thermal, and Morphological Properties of Carbon Black Filled Poly(Propylene)

**Anesh Manjaly Poulose,[1] Arfat Anis,[1] Hamid Shaikh,[1] Justin George,[2] Saeed M. Al-Zahrani[1]**
[1]*Chemical Engineering Department, King Saud University, Riyadh, Saudi Arabia*

[2]*Department of Civil Engineering, Center of Excellence for Concrete Research and Testing, King Saud University, Riyadh, Saudi Arabia*

**Poly(propylene) (PP)/carbon black (CB) composites are melt-blended in a Brabender mixer with varying CB content. With the special-grade conductive CB, the surface resistivity of PP/CB composite was reduced by 13 orders of magnitudes by increasing the CB content from 0 to 15 wt%. The plasticizer poly(ethylene glycol) di-methyl ether (PEGDME) is used (0–5 wt%) to improve the dispersion of the CB in the polymer matrix and to reduce the surface resistivity of the composites. But the PEGDME plasticizer used here has no positive effect on the surface resistivity of the composites; in fact, it enhances the surface resistivity value by one order of magnitude at higher concentration (5 wt%). The scanning electron microscopy (SEM) pictures indicate that the presence of foreign material (plasticizer) especially at higher concentration disrupts the continuous carbon network inversely affecting the conductivity values. Finally, the optimization of the input variables (CB and PEGDME loading) is done using the design of experiment approach. POLYM. COMPOS., 00:000–000, 2015. © 2015 Society of Plastics Engineers**

## INTRODUCTION

Carbon-filled polymer composites (CPCs) have superior electrical and thermal conductivity, improved physical properties, and resistance to corrosive chemicals when compared to metals and metal-filled polymers. Different types of carbon fillers such as single-walled and multi-walled carbon nanotubes (SWCNTs and MWCNTs) [1–9], carbon black (CB) [10–18], carbon fiber [19, 20], graphene [21–24], graphite and graphite derivatives [25–27] are reported in the literature to meet the required electrical and mechanical properties. These composites find applications in antistatic and electrostatic dissipation materials, positive temperature coefficient materials, electromagnetic interference shielding, and in semiconducting layers to prevent the discharge [28, 29].

The conductivity of the CPCs increases significantly when the conductive filler forms a continuous network in the matrix; this process is called percolation and can be explained by the percolation theory [30]. The material behaves as an insulator below the so-called percolation threshold and as a conductor above this threshold due to the formation of an infinite conducting network in the matrix. The percolation threshold and the conductivity of the CPCs mainly depend on the dispersion of the conductive fillers in the polymer matrix. The main challenges meet in the CPC processing are its high melt viscosity, strong tendency of the carbon particles to form the aggregates inversely affecting the electrical conductivity [31, 32]. The efforts have been made and are reported in literature to minimize the aggregation of carbon based fillers [33–40]. The effect of different processing parameters such as mixing temperature, screw speed, and residence time on the dispersion of carbon fillers and on the conductivity of the CPCs are reported in literature [6, 33, 34]. They have shown that the mixing conditions has crucial role on the dispersion and distribution of conducting fillers in the matrix and on the conductivity values. The effect of polymer matrix viscosity on the dispersion of carbon nanotubes (CNTs) and on the conductivity of the composites is also studied [35]. The results reveal that the lowest percolation thresholds are found in the composites based on the low viscosity matrix as the CNT agglomerate dispersion is increased with increasing matrix viscosity due to the higher input of mixing energy. Other methods such as step-wise mixing and master batch dilution procedure are tried to minimize the agglomeration of carbon fillers in the matrix [36]. The techniques like solid-state shear pulverization followed by melt mixing [37] and solid-state mechano-chemical pulverization process [38] are also implied in PP/CNT composites. Chemical methods such as CNT functionalization [39, 40], CNT surface treatment with

*Correspondence to*: Anesh Manjaly Poulose; e-mail: apoulose@ksu.edu.sa
DOI 10.1002/pc.23834
Published online in Wiley Online Library (wileyonlinelibrary.com).

TABLE 1. Composition details of the polymer composites.

| Sample name | Composition details |
|---|---|
| PP | Poly(propylene) + 0 wt% CB + 0 wt% PEGDME |
| PP-5CB-0 PEGDME | Poly(propylene) + 5 wt% CB + 0 wt% PEGDME |
| PP-10CB-0 PEGDME | Poly(propylene) + 10 wt% CB + 0 wt% PEGDME |
| PP-15CB-0 PEGDME | Poly(propylene) + 15 wt% CB + 0 wt% PEGDME |
| PP-5CB-2.5 PEGDME | Poly(propylene) + 5 wt% CB + 2.5 wt% PEGDME |
| PP-10CB-2.5 PEGDME | Poly(propylene) + 10 wt% CB + 2.5 wt% PEGDME |
| PP-15CB-2.5 PEGDME | Poly(propylene) + 15 wt% CB + 2.5 wt% PEGDME |
| PP-5CB-5 PEGDME | Poly(propylene) + 5 wt% CB + 5 wt% PEGDME |
| PP-10CB-5 PEGDME | Poly (propylene) + 10 wt% CB+ 5wt % PEGDME |
| PP-15CB-5 PEGDME | Poly (propylene) + 15 wt% CB + 5 wt% PEGDME |

strong acid mixture followed by treatment with poly(ethylene glycol) (PEG) [41], surface treatment of CNT via gliding arc plasma [42], and PEG as additive in MWCNT/linear low density polyethylene (LLDPE) [43], MWCNT/polylactic acid (PLA) [44] PLA/CB [17] composites are also reported to minimize the agglomeration of carbon-based fillers in the matrix.

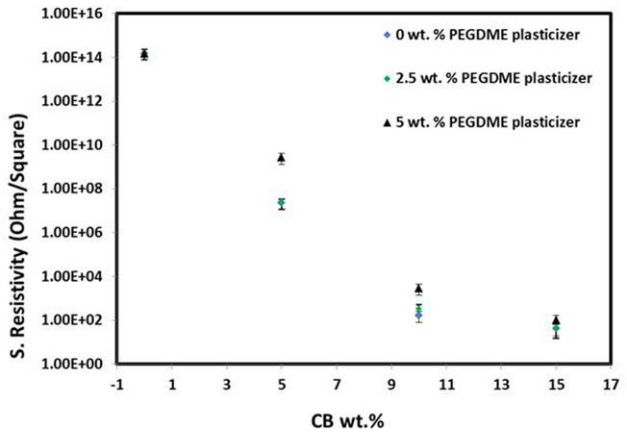


FIG. 1. Surface resistivity plot of poly(propylene)/carbon black composites. [Color figure can be viewed in the online issue, which is available at wileyonlinelibrary.com.]

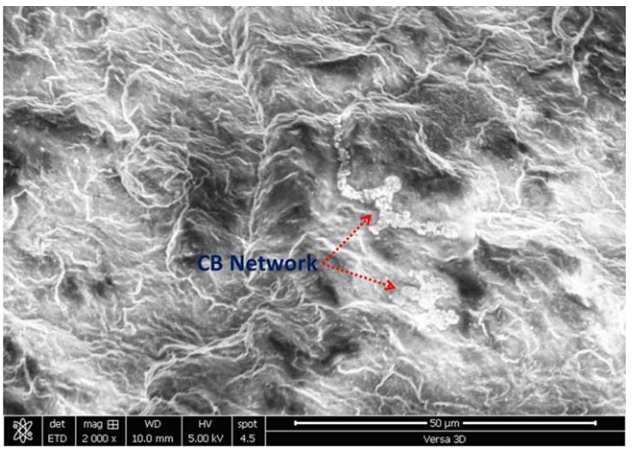


FIG. 2. SEM on PP + 5 wt% CB + 0 wt% PEGDME. [Color figure can be viewed in the online issue, which is available at wileyonlinelibrary.com.]

In this article, the CB has been chosen as a conductive particle in PP matrix as it is effective, comparatively cheap, and is easily available. The electrical properties of CPCs with CB are greatly affected by the CB properties, including its aggregate structure, particle size, specific surface area, and surface chemistry [45]. The low surface area special-grade conductive CB under the trade name

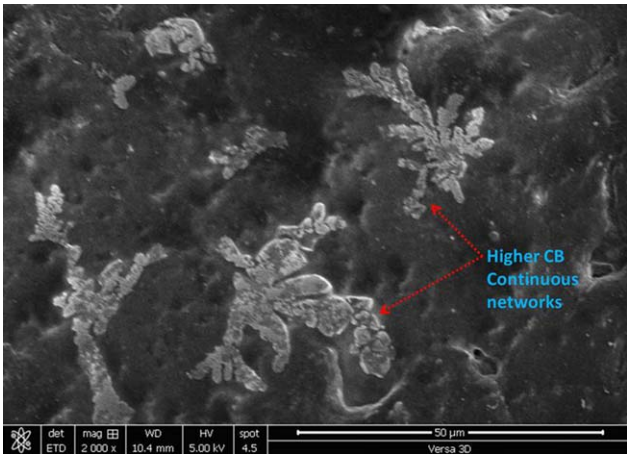


FIG. 3. SEM on PP + 15 wt% CB + 0 wt% PEGDME. [Color figure can be viewed in the online issue, which is available at wileyonlinelibrary.com.]

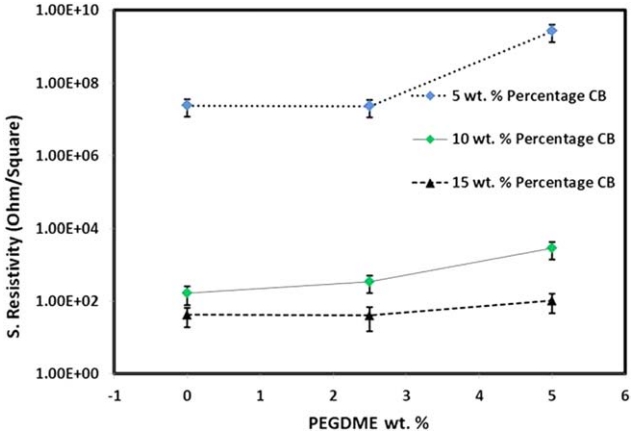


FIG. 4. Surface resistivity plot of poly(propylene)/carbon black composites (carbon black wt. percentage kept constant varying PEGDME wt%). [Color figure can be viewed in the online issue, which is available at wileyonlinelibrary.com.]

 DOI 10.1002/pc

TABLE 2. Surface resistivity values of poly(propylene)/carbon black composites.

| 0 wt % PEGDME | | 2.5 wt% PEGDME | | 5 wt% PEGDME | |
|---|---|---|---|---|---|
| CB wt% [Vol%] | Surface resistivity (Ohm/Square) [STDEV] | CB wt% [Vol%] | Surface resistivity (Ohm/Square) [STDEV] | CB wt% [Vol%] | Surface resistivity (Ohm/Square) [STDEV] |
| 0 [0] | 1.54E+14 [0] | 0 [0] | 1.54E+14 [0] | 0 [0] | 1.54E+14 [0] |
| 5 [20.9] | 2.40E+07 [0] | 5 [20.6] | 2.28E+07 [0] | 5 [20.3] | 2.70E+09 [0] |
| 10 [34.6] | 1.67E+02 [3.7] | 10 [34.2] | 3.42E+02 [0.8] | 10 [33.7] | 3.11E+03 [4.9] |
| 15 [44.3] | 4.22E+01 [1.5] | 15 [43.8] | 4.15E+01 [3.7] | 15 [43.3] | 1.05E+02 [4.2] |

TABLE 3. Surface resistivity data of poly(propylene)/carbon black composites.

| 5 wt% Carbon black | | 10 wt% Carbon black | | 15 wt% Carbon black | |
|---|---|---|---|---|---|
| PEGDME wt% [Vol%] | Surface resistivity (Ohm/Square) [STDEV] | PEGDME wt% [Vol%] | Surface resistivity (Ohm/Square) [STDEV] | PEGDME wt% [Vol%] | Surface resistivity (Ohm/Square) [STDEV] |
| 0 [0] | 2.40E+07 [0] | 0 [0] | 1.67E+02 [3.7] | 0 [0] | 4.22E+01 [1.5] |
| 2.5 [1.6] | 2.28E+07 [0] | 2.5 [1.3] | 3.42E+02 [0.8] | 2.5 [1.2] | 4.15E+01 [3.7] |
| 5 [3.2] | 2.70E+09 [0] | 5 [2.7] | 3.11E+03 [4.9] | 5 [2.3] | 1.05E+02 [4.2] |

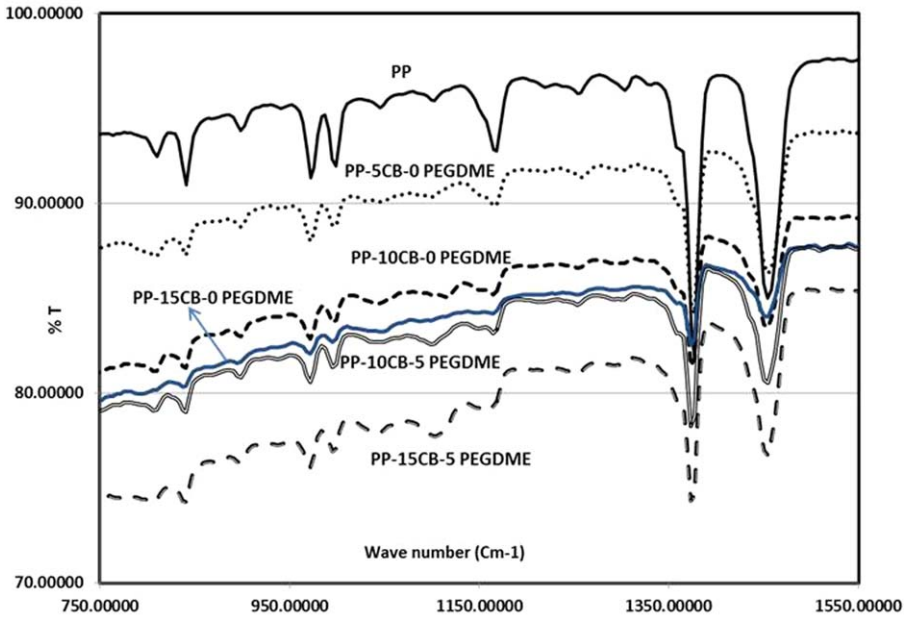


FIG. 5. ATR–FTIR spectroscopy on poly(propylene), PP/CB composites, and PEGDME plasticized samples (750–1550 $cm^{-1}$). [Color figure can be viewed in the online issue, which is available at wileyonlinelibrary.com.]

Ensaco 250G is used for the present study. It is well known that the dispersion of the carbon particles in the polymer matrix is the deciding factor for the conductivity of the composites and in this scenario a known plasticizer is used to improve the dispersion of CB in the PP matrix.

## EXPERIMENTAL

### *Materials and Methods*

PP is supplied by TASNEE under the trade name TASNEE PP H4120 with a melt flow rate (MFR) of 12 g/10 min (ISO 1133) and density of 0.9 $g/cm^3$. The special-grade conductive CB under the trade name Ensaco 250G is supplied by TIMCAL. It has a Brunauer Emmett Teller (BET) nitrogen surface area of 65 $m^2/g$, pour density of 170 $kg/m^3$, and volume resistivity of $10^3$ ohm cm (TIMCAL method 11).

The plasticizer used in this work is poly(ethylene glycol) di-methyl ether (PEGDME) supplied by Aldrich Company and has a number average molecular weight of $M_n \sim 1{,}000$. All the composites have been melt-mixed in a Brabender mixer; Polylab QC at a temperature of 190–200°C for a mixing time of 3 min at 40 rpm. The composition details of the polymer composites prepared for the study are shown in Table 1.

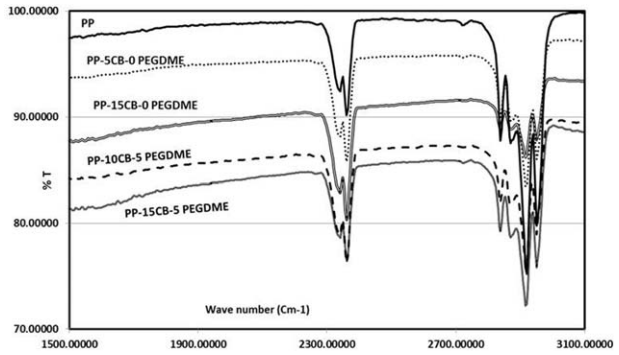


FIG. 6. ATR–FTIR spectroscopy on poly(propylene), PP/CB composites, and PEGDME plasticized samples (1500–3100 cm-1).

The melt mixed material from Haake are compressed in COLLIN press into a sheet (8 × 8 × 0.3 cm) for the surface resistivity measurements. The compression molding is done at a temperature of 220°C under 100 bar pressure and a holding time of 3 min.

For high-resistivity plastic materials, the resistivity measurements are made using a Keithley resistivity meter (Model 6517 A) coupled with a resistivity chamber (Model 8009) according to ASTM D257. For low-resistivity materials, that is, conductive plastics, resistivity measurements are made using a low-resistivity meter (Loresta-GP, Mitsubishi, Japan) coupled with an ESP-type four probe (model MCP-TP08P). Three specimens of each sample were taken for measurement in order to ensure the repeatability and reproducibility of result. Each value obtained is the average of three measurements performed on each specimen.

The attenuated total reflectance Fourier transform infrared spectroscopy (ATR-FTIR) spectrum analysis is carried out in a Thermo Scientific Nicolet iN10 FTIR microscope having a Germanium micro tip ATR accessory (400–4000 $cm^{-1}$).

The secondary electron images are taken using an FE-SEM, Model; FEI-Versa 3D with an accelerating energy of 5 kV.

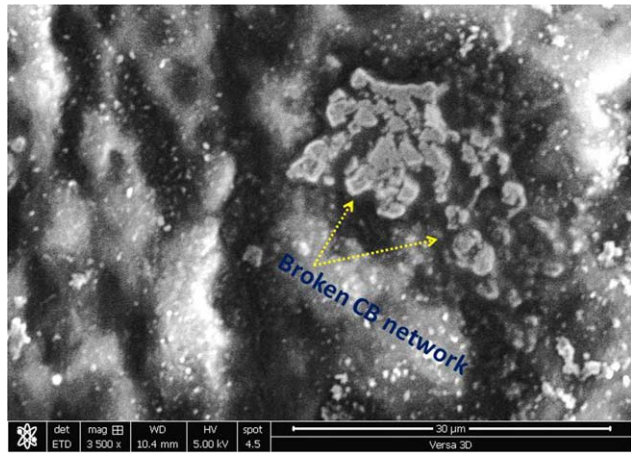


FIG. 8. SEM on PP + 15 wt% CB +5 wt% PEGDME. [Color figure can be viewed in the online issue, which is available at wileyonlinelibrary.com.]

The differential scanning calorimetry (DSC) measurements are carried out in Shimadzu DSC-60. The heating and cooling program is from 30°C to 220°C at a rate of 10°C/min and the holding time of 4 min.

Design of experiment (DOE) studies is performed using Design Expert software (Version 9, Stat-Ease). The most popular response surface method (RSM) design is the central composite design (CCD). A two-level factorial design was utilized in this study with two independent variables namely the CB and the plasticizer composition. Response surface methodology (RSM) is an effective tool for optimizing the desired process response by understanding the influence of the process variable and their interactions. The statistical analysis of the model is performed by analysis of variance (ANOVA).

## RESULTS AND DISCUSSION

### *Surface Resistivity Measurements*

Figure 1 and Table 2 show the surface resistivity data as a function of the CB content for the PP/CB composite

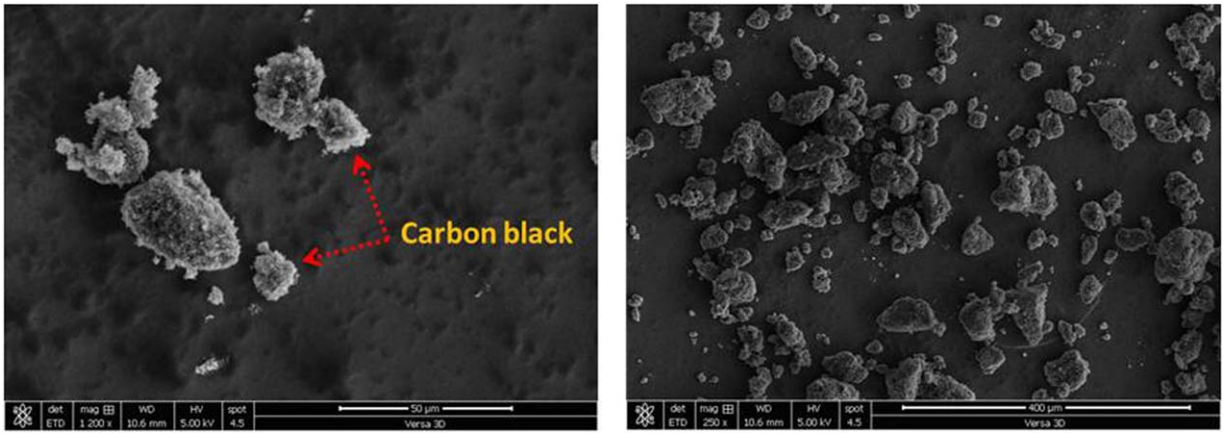


FIG. 7. SEM on carbon black (Ensaco 250G) at different magnifications. [Color figure can be viewed in the online issue, which is available at wileyonlinelibrary.com.]

 DOI 10.1002/pc

TABLE 4. DSC data of poly(propylene)/carbon black composites (data taken from the second heating and cooling).

| Sample | $T_m$ (°C) | $T_c$ (°C) | $\Delta HT_m$ (J/g) | $\Delta HT_c$ (J/g) | Crystallinity (%) |
|---|---|---|---|---|---|
| Poly(propylene) + 0 wt.% CB + 0 wt% PEGDME | 165.0 | 121.2 | 95.1 | 89.9 | 45.9 |
| Poly(propylene) + 5 wt% CB + 0 wt.% PEGDME | 165.3 | 121.1 | 82.7 | 80.8 | 40.0 |
| Poly(propylene) + 5 wt% CB + 2.5 wt% PEGDME | 165.0 | 120.8 | 76.3 | 80.6 | 36.9 |
| Poly(propylene) + 5 wt% CB + 5 wt% PEGDME | 166.3 | 120.7 | 72.2 | 76.0 | 34.9 |
| Poly(propylene) + 10 wt% CB + 0 wt% PEGDME | 166.0 | 121.6 | 76.8 | 81.0 | 37.1 |
| Poly(propylene) + 10 wt% CB + 2.5 wt% PEGDME | 164.5 | 120.0 | 66.2 | 76.0 | 32.0 |
| Poly(propylene) + 10 wt% CB + 5 wt% PEGDME | 164.6 | 120.7 | 72.3 | 77.3 | 34.9 |
| Poly(propylene) + 15 wt% CB + 0 wt% PEGDME | 165.6 | 121.9 | 64 | 74.8 | 31.0 |
| Poly(propylene) + 15 wt% CB + 2.5 wt% PEGDME | 164.3 | 120.2 | 65.6 | 74.4 | 31.7 |
| Poly(propylene) + 15 wt% CB + 5 wt% PEGDME | 164.2 | 120.1 | 68.9 | 74.6 | 33.3 |

keeping the plasticizer content constant. As shown in Fig. 1, the room temperature surface resistivity of PP/CB composite decreased sharply with increasing CB content ($10^{+14}$ to $10^{+1}$ Ohm/Square as CB percentage increases from 0 to 15 wt%). A significant drop in surface resistivity ($10^{+9}$ to $10^{+3}$ Ohm/Square) is achieved on increasing the CB content from 5 to 10 wt%. Thus, for PP/CB composites one can say that the percolation threshold lies in between 5 and 10 wt% CB. The formation of continuous conducting paths in the PP matrix is confirmed from the SEM pictures (Figs. 2 and 3). The higher CB network density is responsible for lowering the surface resistivity values from 5 to 15 wt% CB and can be clearly visible from SEM pictures (Figs. 2 and 3). The models for the filler network formation and evolution are reported in the previous studies [46]. After the percolation is achieved, the surface resistivity of the PP composites does not greatly change with increasing filler content.

The PEGDME plasticizer used here has no significant effect on the conductivity of the composites; in fact, the higher plasticizer content (5 wt%) drops the conductivity of the composites by one order of magnitude. The negative effect of 5 wt% PEGDME plasticizer on the conductivity of PP/CB composite can be clearly seen from Table 3 and Fig. 4. As shown in Fig. 4, the effect is more visible in 5 wt% CB sample as there is pronounced increase in the surface resistivity values from 0 to 5 wt% of PEGDME plasticizer. As shown in Fig. 4, the negative effect of the plasticizer on the conductivity decreases on increasing the CB content, that is, The slope of surface resistivity increment decreases with increasing the CB content.

To understand the negative effect of plasticizer content (5 wt%) on the surface resistivity of PP/CB composites, ATR–FTIR and SEM scans are carried out (Figs. 2, 3, 5–8). The ATR–FTIR (750–3100 $cm^{-1}$) spectra (Figs. 5 and 6) of PP, the PP/CB, and the plasticized composites are identical and confirmed that the plasticizer is not chemically linked to the polymer matrix and the possibility of co-polymerization is excluded. On comparing the SEM in Figs. 3 and 8, it is evident that the presence of foreign material (plasticizer) especially at higher concentration somehow disrupts the continuous carbon network inversely affecting the conductivity values.

### *The Plasticizer and CB on the Thermal Behavior of PP/CB Composites*

The CB used here has no effect on the crystallization temperature ($T_c$) and melting temperature ($T_m$) of the composites; in fact, it has negative effect on the $\Delta HT_m$ and $\Delta HT_c$ values (Table 4). These results indicate that the addition of CB marginally diminishes the crystallization rate of PP matrix and the total crystallinity of the composites as shown in Table 4. The total crystallinity is calculated based on the equation $(\Delta HT_m/\Delta H^0T_m) \times 100$ [$\Delta H^0T_m$ for PP is reported as 207 J/g] [47]. The decrease in crystallinity of PP-filled with CB can be due to the agglomerations of CB which restrict the molecular movement and hinder the orderly packing of molecular segments of PP matrix [48]. In fact, the decrease in the crystallinity of the PP matrix with PEGDME plasticizer is less on comparison with PP/CB without plasticizer.

### *The Design of Experiment (DOE) Results*

The CCD is a powerful statistical approach to model and optimize the required properties of a composite influenced by several independent variables [49–52]. The surface resistivity response data is added to the CCD matrix design generated by design expert software as shown in Table 5. Further analysis is done using the software to optimize the variables for achieving minimum surface resistivity.

The model is selected on the basis that has insignificant lack of fits. For this test, the software suggests quadratic model for this analysis having maximum degree of freedom and sum of square values. Table 6 shows the model summary statistics which is the confirmation of linear model. The ANOVA for Response Surface Quadratic model is shown in Table 7. The basis of selecting this model was the maximum value of "Predicted R-Squared" and considerably higher value of "Adjusted R-Squared." The adjusted and predicted $R$ values for the lack of fit tests are mentioned in Table 6.

TABLE 5. Central composite design matrix model generated by Design-Expert software.

| Run | CB loading (wt%) [Vol%] | PEGDME loading (wt%) [Vol%] | Surface resistivity (Ohm/square) [STDEV] |
|---|---|---|---|
| 1 | 10 [34.2] | 2.5 [1.3] | 341 [0.8] |
| 2 | 5 [20.3] | 5 [3.2] | 2.7E+009 [0] |
| 3 | 5 [20.6] | 2.5 [1.6] | 2.28E+007 [0] |
| 4 | 15 [43.8] | 2.5 [1.2] | 41.5 [3.7] |
| 5 | 10 [34.2] | 2.5 [1.34] | 340.8 [0.8] |
| 6 | 15 [43.3] | 5 [2.3] | 105 [4.2] |
| 7 | 10 [34.2] | 2.5 [1.34] | 342 [0.8] |
| 8 | 15 [44.3] | 0 [0] | 42.2 [1.5] |
| 9 | 10 [33.7] | 5 [2.7] | 3110 [4.9] |
| 10 | 10 [34.6] | 0 [0] | 167 [3.7] |
| 11 | 10 [34.2] | 2.5 [1.34] | 342.2 [0.8] |
| 12 | 10 [34.2] | 2.5 [1.34] | 342.1 [0.8] |
| 13 | 5 [20.9] | 0 [0] | 2.4E+007 [0] |

The model $F$ value of 372.55 means the model is significant. There is only 0.01% chance that the $F$ value this large could occur due to noise. The value "Prob $>$ $F$" less than 0.0500 indicate the model terms are significant. In this case, the terms $A$, $B$, AB, $A^2$, $B^2$ are significant model terms. When the values ARE greater than 0.1000, it indicates that the model terms are insignificant. If there are many insignificant model terms, then the model reduction may improve the model. The "Lack of Fit $F$-value" of 140097.57 means the lack of fit is significant (Table 7). There is only 0.01% that the "Lack of Fit $F$-value" this large could occur due to noise.

The following second order Eq. *1* in terms of actual parameters was obtained.

$$\text{Surface resistivity} = 5.74 - 7.26A + 1.43B - 0.95\text{AB} + 4.84A^2 + 1.08B^2 \quad (1)$$

where $A$ is CB loading and $B$ is PEGDME loading.

The model equation allows to confidently predicting the surface resistivity within the design area. It was observed that the resistivity of the composites decreases with increase in the CB content, whereas the PEGDME content has a negative effect. The model terms attained for both input variables are found to be significant. The 3D surface graph showing the combination of CB and PEGDME loading is shown in the Fig. 9. The figure indicates that the increase in the CB content of the composites even at zero PEGDME content decreases the surface resistivity of the composites.

The optimization of the input variables (keeping the CB in range and PEGDME loading minimum) is very important to get the minimum surface resistivity and is shown in Table 8. The optimized composition was found to be 13.25 wt% CB loading and 0 wt% PEGDME loading to achieve the minimum surface resistivity in the composites. At this optimum composition, the predicted surface resistivity by the model was found to be 31.452 Ohms/square, whereas the actual value was observed to be 34.173 Ohms/square. The predicted and the actual surface resistivity values for the optimized composition was found to be in good agreement and hence confirmed that this model is a good predictor of the response.

## CONCLUSIONS

The PP/CB composites are melt mixed with varying CB filler content. It is found that the surface resistivity value significantly reduces ($10^{+14}$ to $10^{+1}$ Ohm/Square)

TABLE 6. Model summary statistics for various polynomial degrees.

| Source | Std. deviation | R-Squared | Adjusted R-Squared | Predicted R-Squared | Press | |
|---|---|---|---|---|---|---|
| Linear | 3.12 | 0.7709 | 0.7251 | 0.5199 | 204.30 | |
| 2FI | 3.23 | 0.7795 | 0.7060 | −0.0565 | 449.52 | |
| Quadratic | 0.48 | 0.9963 | 0.9936 | 0.9645 | 15.09 | Suggested |
| Cubic | 0.26 | 0.9992 | 0.9981 | 0.9087 | 38.84 | Aliased |

TABLE 7. ANOVA for Response Surface Quadratic model.

| Source | Sum of Squares | Degree of freedom | Mean square | $F$-value | Prob $>$ $F$ | |
|---|---|---|---|---|---|---|
| Model | 423.90 | 5 | 84.78 | 372.55 | <0.0001 | Significant |
| A-CB Loading | 315.81 | 1 | 315.81 | 1387.80 | <0.0001 | |
| B-PEGDME Loading | 12.21 | 1 | 12.21 | 53.65 | 0.0002 | |
| AB | 3.63 | 1 | 3.63 | 15.96 | 0.0052 | |
| $A^2$ | 64.60 | 1 | 64.60 | 283.88 | <0.0001 | |
| $B^2$ | 3.24 | 1 | 3.24 | 14.22 | 0.0070 | |
| Residual | 1.59 | 7 | 0.23 | | | |
| Lack of fit | 1.59 | 3 | 0.53 | 1.401E+005 | <0.0001 | Significant |
| Pure error | 1.516E-005 | 4 | 3.790E-006 | | | |
| Cor total | 425.49 | 12 | | | | |


DOI 10.1002/pc

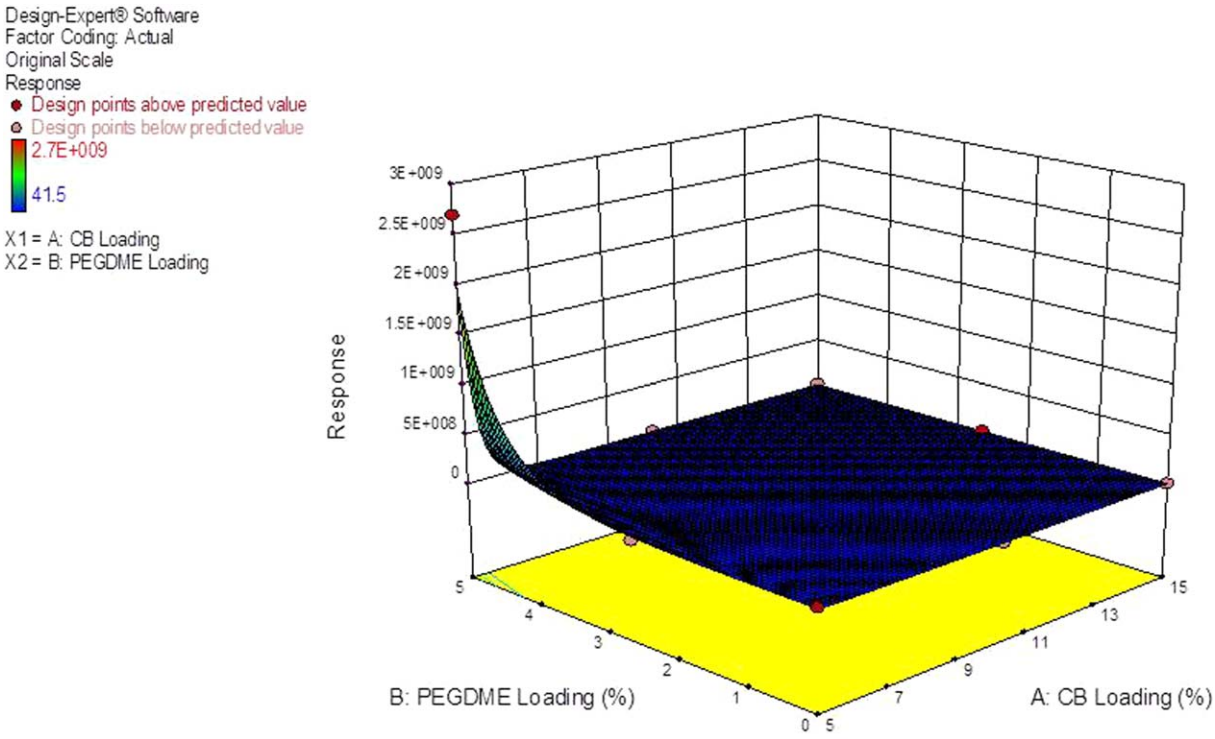


FIG. 9. The 3D surface graph showing the effect of CB and PEGDME loading. [Color figure can be viewed in the online issue, which is available at wileyonlinelibrary.com.]

TABLE 8. Optimization of the variables (CB and PEGDME loading) using the model.

| Constraints | | | | | | |
|---|---|---|---|---|---|---|
| Name | Goal | Lower limit | Upper limit | Lower weight | Upper weight | Importance |
| A:CB Loading | Is in range | 5 | 15 | 1 | 1 | 3 |
| B:PEGDME Loading | Minimize | 0 | 5 | 1 | 1 | 3 |
| Response | Minimize | 41.5 | 2.7E+009 | 1 | 1 | 5 |

| Selected Solution | | | |
|---|---|---|---|
| CB loading | PEGDME loading | Response | Desirability |
| 13.250 | 0.000 | 31.452 | 1.000 |

on increasing the CB percentage in the matrix (0–15 wt%). The percolation threshold of PP/CB composites lies in between 5 and 1 wt% CB and with further increase in the filler content surface resistivity value improves only marginally. The thermal analysis of the composites indicates that the addition of CB marginally diminishes the crystallization rate of PP and the total crystallinity of the composites.

The PEGDME plasticizer has been tried to improve the dispersion of CB in the matrix and hence the conductivity of PP/CB composites. The results shown that the plasticizer has no effect on this particular system in fact it reduce the conductivity value by one order of magnitude at higher concentration. The presence of foreign material (plasticizer) especially at higher concentration disrupts the continuous carbon network inversely affecting the conductivity values. By using the DOE modeling, the optimized composition for the minimum surface resistivity was found to be 13.25 wt% CB loading and 0 wt% PEGDME.

## ACKNOWLEDGEMENT

The authors would like to extend their sincere appreciation to the Deanship of Scientific Research at King Saud University for its funding of this research through the Research Group Project No. RG 1435-015.

## REFERENCES

1. F.Y. Castillo, R. Socher, B. Krause, R. Headrick, B.P. Grady, R.P. Silvy, and P. Potschke, *Polymer*, **52**, 3835 (2011). [CrossRef][10.1016/j.polymer.2011.06.018

2. A. Gupta and V. Choudhary, *J. Mater. Sci*., **48**, 3347 (2013).
3. A. Huegun, M. Fernandez, M.E. Munoz, and A. Santamaria, *Compos. Sci. Technol*., **72**, 1602 (2012).
4. D.W. Kang and S.H. Ryu, *Polym. Int*., **62**, 152 (2013).
5. K. Madhukar, A.V.S. Sainath, B.S. Rao, D.S. Kumar, N. Bikshamaiah, Y. Srinivas, N. Mohan Babu, and B. Ashok, *Polym. Eng. Sci*., **53**, 397 (2013).
6. S. Maiti, N.K. Shrivastava, S. Suin, and B.B. Khatua, *Express Polym. Lett*., **7**, 505 (2013).
7. K. Mezghani, M. Farooqui, S. Furquan, and M. Atieh, *Mater. Lett*., **65**, 3633 (2011).
8. I. Dubnikova, E. Kuvardina, V. Krasheninnikov, S. Lomakin, I. Tchmutin, and S. Kuznetsov, *J. Appl. Polym. Sci*., **117**, 259 (2010).
9. M.A.L. Manchado, L. Valentini, J. Biagiotti, and J.M. Kenny, *Carbon*, **43**, 1499 (2005).
10. S.A.H. Pour, B. Pourabbas, and M.S. Hosseini, *Mater. Chem. Phys*., **143**, 830 (2014).
11. S. Huang, Z. Liu, C. Yin, Y. Wang, Y. Gao, C. Chen, and M. Yang, *Macromol. Mater. Eng*., **297**, 51 (2012).
12. S. Huang, Z. Liu, S. Zheng, and M. Yang, *Colloid Polym. Sci*., **291**, 3005 (2013).
13. A. Kasgoz, D. Akın, and A. Durmus, *Compos. Part B: Eng*., **62**, 113 (2014).
14. S.A.E. Kassim, M.E. Achour, L.C. Costa, and F. Lahjomri, *J. Electrostat*., **72**, 187 (2014).
15. X. Liu, J. Kruckel, G. Zheng, and D.W. Schubert, *Compos. Sci. Technol*., **100**, 99 (2014).
16. S. Zheng, S. Huang., D. Ren, W. Yang, Z. Liu, and M. Yang, *J. Appl. Polym. Sci*., **131**, 40686 (2014).
17. Z. Su, K. Huang, and M. Lin, *J. Macromol. Sci. Phys*., **51**, 1475 (2012).
18. C.L. Yin, Z.Y. Liu, S.L. Huang, C. Chen, and M.B. Yang, *J. Macromol. Sci. Phys*., **52**, 762 (2013).
19. L. Shen, F.Q. Wang, H. Yang, and Q.R. Meng, *Polym. Test*., **30**, 442 (2011).
20. S. Zhao, H. Zhao, G. Li, K. Dai, G. Zheng, C. Liu, and C. Shen, *Mater. Lett*., **129**, 72 (2014).
21. Y. Li, J. Zhu, S. Wei, J. Ryu, L. Sun, and Z. Guo, *Macromol. Chem. Phys*., **212**, 1951 (2011).
22. M.A. Milani, R. Quijada, N.R.S. Basso, A.P. Graebin, and G.B. Galland, *J. Polym. Sci. Part A: Polym. Chem*., **50**, 3598 (2012).
23. V.P. Sergey, P.M. Nedorezova, A.N. Klyamkina, A.A. Kovalchuk, A.M. Aladyshev, A.N. Shchegolikhin, V.G. Shevchenko, and V.E. Muradyan, *J. Appl. Polym. Sci*., **127**, 904 (2013).
24. Y.V. Syurik, M.G. Ghislandi, E.E. TKalya, G. Paterson, D. McGrouther, O.A. Ageev, and J. Loos, *Macromol. Chem. Phys*., **213**, 1251 (2012).
25. R.A. Shanks and F.T. Cerezo, *Composites Part A*, **43**, 1092 (2012).
26. P. Steurer, R. Wissert, R. Thomann, and R. Mulhaupt, *Macromol. Rapid Commun*., **30**, 316 (2009).
27. C. Du, P. Ming, M. Hou, J. Fu, Y. Fu, X. Luo, Q. Shen, Z. Shao, and B. Yi, *J. Power Sources*, **195**, 5312 (2010).
28. R. Sanjines, M.D. Abad, R.Cr. Vaju, M. Smajda, and A. Mionic, Magrez, *Surf. Coat. Technol*., **206**, 727 (2011).
29. L. Feng, N. Xie, and J. Zhong, *Materials*, **7**, 3919 (2014).
30. D. Stauffer and A. Aharony, Introduction To to Percolation Theory, Taylor and Francis, London (1994).
31. G.R. Kasaliwal, S. Pegel, A. Goldel, P. Potschke, and G. Heinrich, *Polymer*, **51**, 2708 (2010).
32. M.H. Al-Saleh and U. Sundararaj, *Polymer*, **51**, 2740 (2010).
33. B.T. Pankaj, R.B. Arub, and R.K. Ajit, *J. Appl. Polym. Sci*., **127**, 1017 (2013).
34. B. Krause, P. Pötschke, and L. Haubler, *Compos. Sci. Technol*., **69**, 1505 (2009).
35. R. Socher, B. Krause, M.T. Muller, R. Boldt, and P. Potschke, *Polymer*, **53**, 495 (2012).
36. K. Ke, Y. Wang, K. Zhang, Y. Luo, W. Yang, B.H. Xie, and M.B. Yang, *J. Appl. Polym. Sci*., **125**, E49 (2012).
37. J. Masuda and J.M. Torkelson, *Macromolecules*, **41**, 5974 (2008).
38. H. Xia, Q. Wang, K. Li, and G.H. Hu, *J. Appl. Polym. Sci*., **93**, 378 (2004).
39. P.C. Ma, N.A. Siddiqui, G. Marom, and J.K. Kim, *Composites Part A*, **41**, 1345 (2010).
40. R.M. Novais, F. Simon, M.C. Paiva, and J.A. Covas, *Composites Part A*, **43**, 2189 (2012).
41. S. Yesil and G. Bayram, *J. Appl. Polym. Sci*., **127**, 982 (2013).
42. Z. Luo, X. Cai, R.Y. Hong, J.H. Li, D.G. Wei, G.H. Luo, and H.Z. Li, *J. Appl. Polym. Sci*., **127**, 4756 (2013).
43. M.T. Muller, B. Krause, and P. Potschke, *Polymer*, **53**, 3079 (2012).
44. Z. Shufen, N. Bing, L. Ruihua, and P. Huayan, *J. Appl. Polym. Sci*., **123**, 1843 (2012).
45. L.R. Tan, Y.J. Gao, S.L. Huang, Z.Y. Liu, and M.B. Yang, *Polym. Bull*., **71**, 1403 (2014).
46. R. Danqi, Z. Shaodi, W. Feng, Y. Wei, L. Zhengying, and Y. Mingbo, *J. Appl. Polym. Sci*., **131**, 39953 (2014).
47. R. Paukkeri and A. Lehtinen, *Polymer*, **34**, 4075 (1993).
48. J. Chen, X. Li, and C. Wu, *Polym. J*., **39**, 722 (2007).
49. A.R. Jeefferie, H.A. Sahrim, T.R. Chantara, A.M. Mazlin, Y. Juliana, and M. Noraiham, *J. Appl. Polym. Sci*., **132**, 42199 (2015).
50. R. Stefan, G. Bjorn, K. Sina Gad'on, C. Andreas, and L. Thomas, Gunter, *J. Appl. Polym. Sci*., **132**, 41997 (2015).
51. H.M. Raymond, D.C. Montgomery, and C.M.A. Cook, Response Surface Methodology: Process and Product Optimization Using Designed Experiments, Wiley, New York (2009).
52. S.C. Vipul, K.B. Nishi, and K.C. Swapan, *Indian J. Chem. Technol*., **20**, 121 (2013).

 DOI 10.1002/pc